Development of polymer wicks for the fabrication of bio-medical sensors

Ana C. Martins [a,b], André Moreira [b], Ana V. Machado [a], Filipe Vaz [c], Carlos Fonseca [b,d,*], João M. Nóbrega [a]

[a] Institute for Polymers and Composites/I3N, University of Minho, Campus of Azurém, 4800-058 Guimarães, Portugal

[b] Universidade do Porto, Faculdade de Engenharia, Rua Roberto Frias, s/n, 4200-465 Porto, Portugal

[c] Centro de Física, Universidade do Minho, 4710-057 Braga, Portugal

[d] SEG-CEMUC, Department of Mechanical Engineering, University of Coimbra, Coimbra, Portugal

Keywords:

Bio-electrode
Bioelectric signal
EEG
Polymer wick
Dry electrode

Abstract

Polymer based wicking structures were fabricated by sintering powders of polycarbonate (PC), ultra-high molecular weight polyethylene and polyamide 12, aiming at selecting a suitable material for an innovative electroencephalography (EEG) bio-electrode. Preliminary experiments showed that PC based wicks displayed the best mechanical properties, therefore more detailed studies were carried out with PC to evaluate the influence of powder granulometry and processing parameters (pressure, temperature and time) on the mechanical properties, porosity, mean pore radius and permeability of the wicks. It was concluded that the mechanical properties are significantly enhanced by increasing the processing time and pressure, although at the expense of a significant decrease of porosity and mean pore diameter (and thus permeability), particularly for the highest applied pressures (74 kPa). However, a good compromise between porosity/permeability and mechanical properties could be obtained by sintering PC powders of particle sizes below 500μ m at 165°C for 5 min , upon an applied pressure of 56 kPa . Moreover, PC proved to be chemically stable in contact with an EEG common used disinfectant. Thus, wicking structures with appropriate properties for the

fabrication of reusable bio-electrodes could be fabricated from the sintering of PC powders.

Introduction

Electroencephalography (EEG) is the recording of the brain electrical activity along the scalp [1]. EEG is nowadays the most widely used brain imaging technique. The main areas of EEG application are: (i) sleep monitoring, (ii) clinical diagnosis and (iii) long-term epilepsy monitoring. Currently used electrodes are metallic (silver is the most common metal) and require application of a conductive paste or gel to decrease the skin/electrode impedance and facilitate signal transfer. Their application is thus time-consuming and error-prone. Furthermore, extensive cleaning of skin, hair and equipment is required after the exam. Their counterparts, the so-called dry electrodes, eliminate the need to use gels or pastes but display high skin-electrode impedances, and exhibit high sensitivity to movement artefacts [2-4].

This work aims at developing the material for a conceptually different EEG electrode that will combine the advantages of the "wet" and "dry" sensor systems, while addressing most of their drawbacks. A specifically developed polymer wick will be the core electrode material. Like in a felt-pen, the upper part of the electrode body will work as a moistener reservoir, for electrode autonomy, and the tip will establish the skin contact. Hence, a reliable low impedance electrode-skin

contact will be achieved without the use of gel paste, by the continuous delivery of a small amount of a moistener solution at the electrode/skin contact point. The moistener will be promptly absorbed by skin without spreading, dirtying or damaging the hair.

Wicks are porous structures commonly used to absorb and transport liquids mainly by the action of capillary pressure [5-7]. A good wick material exhibits a high permeability/liquid absorption capacity and can induce significant capillary liquid pressure gradients. However, these two properties oppose to each other: large pores are required for high permeability/liquid absorption, while small pores are needed to induce large capillary pressures; therefore a compromise has to be found to achieve an optimal behaviour. Experience shows that, with an appropriate liquid, reasonable permeability values and capillary action can be obtained with porosities of $50 - 60\%$ and mean pore radius of $5 - 50\mu$ m [7,8].

Porous interconnected polymeric structures have been used in a broad range of applications, from the biomedical area (drug controlled release, scaffolds and support for bimolecular immobilization) to filtration membranes, heat pipes and vapour chambers, sorbents, silencers, fragrance diffusers for perfumes and air fresheners and many other applications [5,6]. However, each application has its own specificities, which may require different fabrication methods. Additive Manufacturing (AM) is a family of recent fabrication techniques that can rapidly produce highly complex three-dimensional physical objects using data generated by CAD systems [9]. These techniques include three-dimensional printing (3D-P), fused deposition modelling (FDM) and selective laser sintering method (SLS) techniques [10-12]. The main advantages of these methods are the high porosity that can be achieved (up to 80%) and the ability to produce materials with controlled pore interconnectivity and pore sizes ranging from 40 to 1000μ m, depending on the particular technique. The SLS and 3D-P techniques originate large pore size distributions [9]. AM methods are in general expensive and time consuming, thus not

suitable for mass production. The rotational moulding is an inexpensive technique but it is only applicable to a narrow range of materials and the final structure shows a high degree of closed pores [13]. The melt moulding process is often used in the microfluidics area and has the advantage of producing structures with independent control of porosity and pore size. Nevertheless, it needs high processing temperatures and residual porogen contamination may occur [14].

On the other hand, chemical methods allow obtaining polymer porous structures with controlled pore size ranging from a few nm to 100μ m, depending on the specific technique and polymer [5]. However, these techniques involve the presence of porogens and other chemicals that must be removed at the end, what has to be carefully addressed for biomedical oriented applications. The same applies to the freeze drying technique, which involves freezing a liquid suspension, followed by the sublimation of the solvent. Highly porous (up to 90% porosity) and interconnected structures are achieved in this case, with pores sizes ranging from tens to a few hundred μm [15].

Finally, the powder sintering technique is a simple and cost-effective technique and it allows the production of interconnected porous structures in a wide range of pore sizes ($1-1000\mu$ m) and porosity (up to 70%), while also offering the possibility of being applied to a large number of polymers. Furthermore it doesn't involve the presence of chemicals. For these reasons it is often preferred for the mass production of wick materials, even in the biomedical area. During this process the powder is compressed and heated at temperatures close to the melting point. The polymer particles will fuse together at their contact surfaces under the effects of applied pressure and temperature, and inter-particle mass-diffusion will occur leading to a solidified body with a complex porous structure and adequate mechanical strength [16-19]. The sintering technique will be used to fabricate the wick electrode porous structures in this work.

Requirements for a porous wick structure to be used as a biopotential electrode

A biopotential electrode based in a polymer wick should stock inside its porous structure a hydrating fluid to be dispensed upon skin contact, so to keep the electrode/skin contact point hydrated for the duration of the exam (some signal acquisitions may last for several hours). Therefore, porosity should be high, but the pore size should be small enough to ensure that the liquid is retained inside the structure. Liquid retention capability also depends on the properties of the hydrating fluid to be used (density and viscosity). Furthermore, the amount of hydrating fluid necessary to decrease the skin impedance is dependent on the person and even environmental conditions. Taking into consideration these variables, the porous structures to be developed should be obtained in a wide range of permeability and porosity values, so the most suitable electrode properties can be adapted in a later stage.

Regarding the required mechanical properties, the force exerted on the electrode is about 3 N , as measured by the authors in a previous work using a Nihon Kohden EEG cap system [3]. If the electrode is of the multipin type, with 24 pins and a 1 mm pin top diameter [20], each pin should be able to safely withstand a pressure of at least 1 MPa . This value

corresponds to the situation where the total force is concentrated on just 25% of the pins, which is considered the worst case scenario. Furthermore, owing to the small pin diameter, the polymer particle size should have a diameter below the 1 mm limit so the structural integrity of the pin does not have to rely on a few interparticle bonds.

Experimental details

Materials

Three different thermoplastic polymers were pre-tested, namely: polycarbonate (PC LEXAN 141R 111, Ge Plastic, MFI = 12 g/10 min at 300°C), ultra-high molecular weight polyethylene (UHMWPE GUR 5113, Ticoma, MFI = 4 g/10 min at 190 °C) and polyamide 12 (PA 12 Rilsan AMNO TLD, Arkema, MFI = 69.4 g/10 min at 235 °C). All polymers were acquired in the form of pellets.

Wick production system

The wick structures were produced using a custom built sintering system. The system produces wicks with 10 mm in diameter and a length ranging between 13 and 23 mm , depending on the applied compression load. It consists of four main components, as illustrated in Fig. 1: the heating resistance which involves the whole cylinder (a), the piston (b), the support for the material (d) and the core cylinder (f). Part (c) ensures that the material is processed in the middle of cylinder (d), part (e) keeps (c) inside the cylinder (d) and (g) orifice to house the thermocouple, Fig. 1 (ii).

The heating resistance (a) is responsible for controlling the system temperature; the core cylinder (f) surrounds all components and distributes the heat generated by the resistance to the material support; the piston (b) is responsible for the raw material compaction and the material support (d) holds the material inside the cylinder during the sintering stage.

The production process starts by heating the system to the predefined processing temperature. After achieving steady state conditions, 1 g of grinded polymer is introduced inside cylinder (d). Then the sample is compressed through the action of the piston, the compression pressure being adjusted by the use of different weights placed on the material support base (b). Once the sintering process is finished, the inner subsystem (Fig. 1 - "b" to "e") is removed and cooled, by immersion in water at room temperature. Finally the wick is collected from the support. Different wicking properties can be achieved by controlling the processing temperature, pressure and time.

Before being processed the polymer pellets are ground to a powder state in a mill in contact with liquid nitrogen. Thereafter, the powders are sieved in order to obtain fractions with different grain sizes, see Table 1.

For the preliminary sintering experiments, aiming at selecting the most suitable polymer, the grain size was set below 500μ m and all materials were processed for 5 min with a pressure of 18.5 kPa and a temperature of 165°C, 125 °C and 160°C for PC, UHMWPE and PA respectively (REF conditions in Table 1). Further processing was carried out with the selected polymer, PC, according with the conditions reported in Table 1.

Characterization of the wick structures

Chemical compatibility with the disinfectant

Polymer films with a thickness of 0.1 mm were fabricated using a hydraulic press (Manual Hydraulic Press, Specac, UK) by applying a 15,000 kg of compression force for 4 min . The processing temperature was set at 250°C for PA and PC and 270°C for UHMWPE. Afterwards, the materials were immersed in a 7.9 g/1 solution of Control III disinfectant (Maril products Inc.) for 3 h . Control III is a commercial disinfectant used for EEG biomedical electrodes. A 10 min immersion is recommended for full disinfection. After immersion the film samples were analysed using a Fourier Transform Infrared Spectrometer (FT/IR - 4100, Jasco) in transmission mode with a 0.4 cm^{-1} resolution.

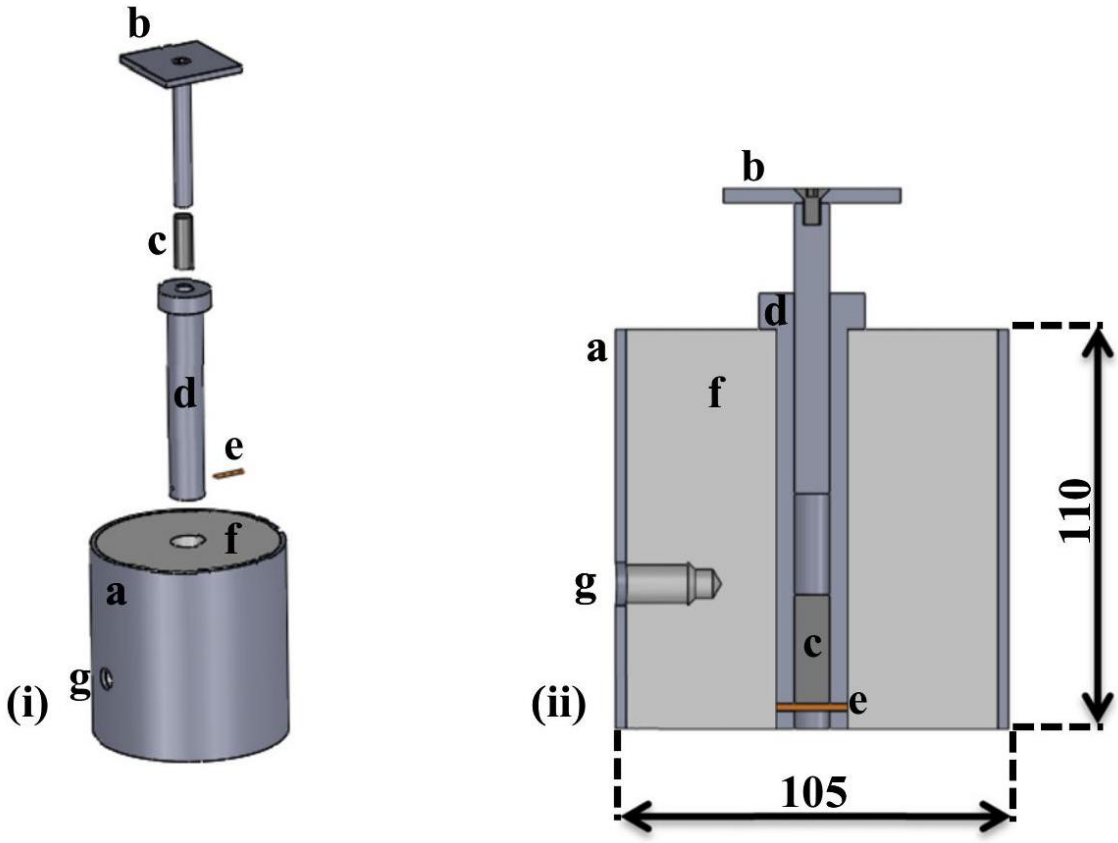

Fig. 1. Sintering system used for the production of PC wicks, comprising: "a": electrical resistance; "b": piston; "c": material support; "d": core cylinder inside which sintering takes place; "e": pin to keep part "c" inside cylinder "d"; "f": heating cylinder; and "g": orifice to house the thermocouple. (i) presents an exploded view of the system and (ii) an assembled cross-section view (dimensions in mm).

Mechanical analysis

The mechanical properties were assessed with a universal tensile testing machine (Instron 4505), working in compression mode. A cross-head speed of 5 mm/min and a load cell of

50 kN were used to obtain the stress-strain curve for each sample. The Young modulus (E) was estimated from the initial slope of the stress-strain curve (linear part of the curve), by linear extrapolation of the tangent to the linear region of the graph, for a 2% strain.

Porosity measurement

The porosity and permeability of the PC porous structures were evaluated by using decane (Decane UN2247, Merck Chemicals) as the test liquid [7]. Four samples were evaluated for each processing condition. The porosity was assessed by two different methods:

- Direct geometric method: The porous volume is calculated from the difference between the geometric volume (V_{geo}) and the effective polymer volume (V_{mat}), calculated from the sample's weight and bulk density. Subsequently, the porous volume (V_{por}) is calculated as: $V_{\text{por}} = V_{\text{geo}} - V_{\text{mat}}$. The result includes open and closed pores.
- Sorptivity method: An analytical balance with an accuracy of 1 mg

Table 1
Sintering process parameters and grain size for the PC powders.

	Time (min)	Pressure (kPa)	Temperature (°C)	Particle size (μm)
REF	5	18.6	165	<500
t_-	2.5	-	-	-
t_+	7.5	-	-	-
2P	-	37.2	-	-
3P	-	55.8	-	-
4P	-	74.4	-	-
T_+	-	-	175	-
T_-	-	-	155	-
G1	-	-	-	100-212
G2	-	-	-	212-306
G3	-	-	-	306-500
G4	-	-	-	500-1000

and a density evaluation kit were used. The wick was suspended in the balance plate by using the density kit and it was slightly submerged in decane. Subsequently, the weight change, resulting from capillary driven liquid absorption, was monitored until saturation was achieved. Since it is assumed that all open pores of the wick were filled with the liquid at the end, the open porosity ε of the wick can be determined by $\varepsilon = m_{\text{sat}} / \left(\rho \pi {R_w}^2 h_f\right)$
where m_{sat} is the mass of absorbed liquid, ρ is the density of decane, R_w is the wick average

pore radius and h_f is the cylindrical sample height [7]. Hence, only the open pores are accounted for by this method.

Permeability and mean pore radius measurement (Darcy law based model)

The permeability K measures the ability of a fluid to flow through the pores or interstices of a material. Specifically, the permeability is a proportionality constant in Darcy's law, relating the pressure gradient to superficial fluid velocity in porous media, $v = K/\mu\nabla P$, where v stands for the superficial fluid velocity, μ is the viscosity and ∇P is the liquid pressure gradient [6]. In this test the wick was fixed to the end of a 30 cm in length rubber nitrile tube to force the liquid through the wick, see Fig. 2. The weight of the released liquid was monitored as a function of time using a balance.

A Darcy's law based model developed by Masoodi et al. [7] was used for the calculation of the permeability of the wicks. According with this model the permeability can be calculated from the straight line defined by Eq. (1), by plotting ln (x_0/x) vs time:

$$\ln\left(\frac{x_0}{x}\right) = \frac{K\rho R_w^2}{\mu L_w R_s^2} t \tag{1}$$

where x_0 and x stand for the initial and actual liquid heights respectively

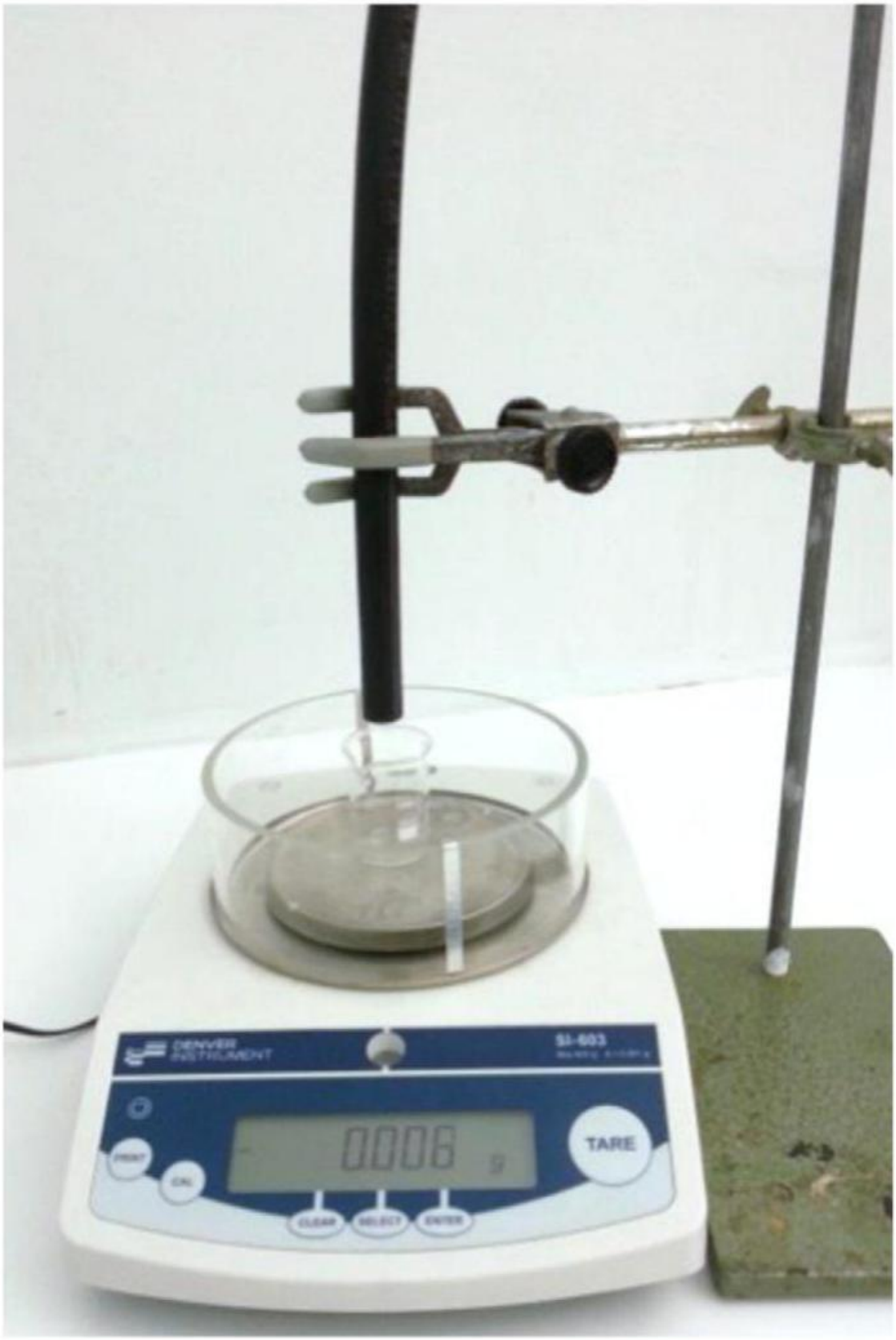
DENVER INSTRUMENT
SI-603
0006
g
TARE
PRINT
CAL
CLEAR
SELECT
ENTER

Fig. 2. Setup developed to measure the permeability and mean pore radius. Adapted from Masoodi et al. [7] setup.
(calculated according with the mass change and the tube diameter), ρ and μ are decanes' density and viscosity, g is the acceleration of gravity, R_w and L_w are the wick radius and length, respectively, t is the time and R_s is the reservoir internal radius. The mean pore radius, R_w, can be calculated from the slope of the straight line defined by Eq. (2) [7]:

$$\ln\left(\frac{x_0 + L_w}{x + L_w}\right) = \frac{\varepsilon R_w^2 R_p^2 \rho g}{8\mu L_w R_s^2} t \quad (2)$$

where ε is the open porosity of the material.

Mercury Intrusion Porosimetry (MIP)

Porosity and pore size distribution were determined by using a MIP AutoPore IV 9500 (Micromeritics) with a pressure up to 228 MPa , enabling determination of a pore-throat diameter down to 5.5 nm .

Scanning electron microscope (SEM)

The samples were observed using a scanning electron microscope (Nova NanoSEM 200, FEI) operating at 5 kV . Before the analysis all samples were immobilized with a graphite tape placed on a metal support and gold-coated.

Statistical data analysis

Statistical analysis in the wick properties upon the variation of the processing parameters was performed by unpaired t-test (with a confidence interval 95%) using GraphPad Prism, version 5.00 software for Windows (GraphPad Software, San Diego, CA, USA). Differences were considered significant at $p < 0.05$. Four samples were tested for each condition.

Results and discussion

Chemical compatibility with the disinfection agent

The FTIR spectra for samples before and after immersion in the disinfectant are shown in Fig. 3. An almost perfect overlapping is observed between the pre- and post-immersion spectra for the three polymers. The spectra of PA 12 display the characteristic double peaks corresponding to C-C bonds in the organic skeleton (~ 2905 and ~ 2838 cm^{-1}) and the two peaks at 1617 and 1535 cm^{-1} attributed to the $N-H$ band (primary amine group). In the PC spectra the band at 1750 cm^{-1} is assigned to the $C=O$ stretching frequency of the carbonate linkage and the characteristic peaks at $\sim 1593, \sim 1490$, and ~ 1470 cm^{-1} are assigned to the $C=Cs$ of the aromatic ring [21]. The UHMWPE entire spectra are dominated by the CH_2 bands, namely at 720 cm^{-1} and 1457 cm^{-1} [22].

Furthermore, PC, PA and UHMWPE samples were weighed on a precision balance before and after the disinfection test. No differences were found between the initial and final mass values, confirming the FTIR conclusions on the chemical stability of all polymers upon disinfection with the selected disinfectant. To note that the polymers underwent a 3 h

immersion test, while only 10 min is recommended for the normal bioelectrode disinfection process.

Effects of the processing conditions and particle size on the properties of the wicks

Preliminary mechanical analysis of the wicks

In order to select the best candidate to produce a polymer wick according to the requirements described in Section 2, a set of preliminary sintering experiments were performed with PC, UHMWPE and PA12 powders with particle diameters set below 500μ m and using the REF condition, as described in Table 1. The yield strength in compression and Young modulus of the porous structures are reported in Table 2.

The results show that the PC-based wick yields the strongest structure and the only one whose yield strength is safely above the 1 MPa threshold defined for the pin mechanical stability. Therefore, PC was chosen as the best candidate for the development of a porous electrode structure.

Mechanical properties

The mechanical parameters of PC porous structures obtained for different processing conditions and powder granulometry are reported in Fig. 4. The processing pressure leads to the highest effects on the mechanical properties, namely an eightfold increase of the Young modulus and yield strength when the pressure increases by a fourfold factor. In fact, higher pressures should enhance the inter-particle contact area and compaction and act as a driving force for mass diffusion, ultimately leading to an improved inter-particle bonding. An improvement of the Young modulus and yield strength is also obtained, although to a lower extent, by increasing either the temperature (80% and 50% increase) or cycle time (3.5 and 6 times increase), as the increase of these parameters leads to faster sintering kinetics. An improvement of the mechanical parameters is also observed with the decrease of PC powder granulometry (50 and 75% respectively, when powder granulometry decreases from G4 to G1, see Table 1), which may be ascribed to the higher inter-particle surface contact area for smaller granulometries, hence enhancing the particles' bonding process.

Porosity

The porosity of the sintered materials was determined from the geometric and sorptivity methods. The first takes account of the total porosity while the second method measures the open porosity only. The influence of the processing conditions on the porosity is reported in Fig. 5. A good agreement exists between both porosity values, meaning that the closed pore volume is negligible. The porosity is mainly affected

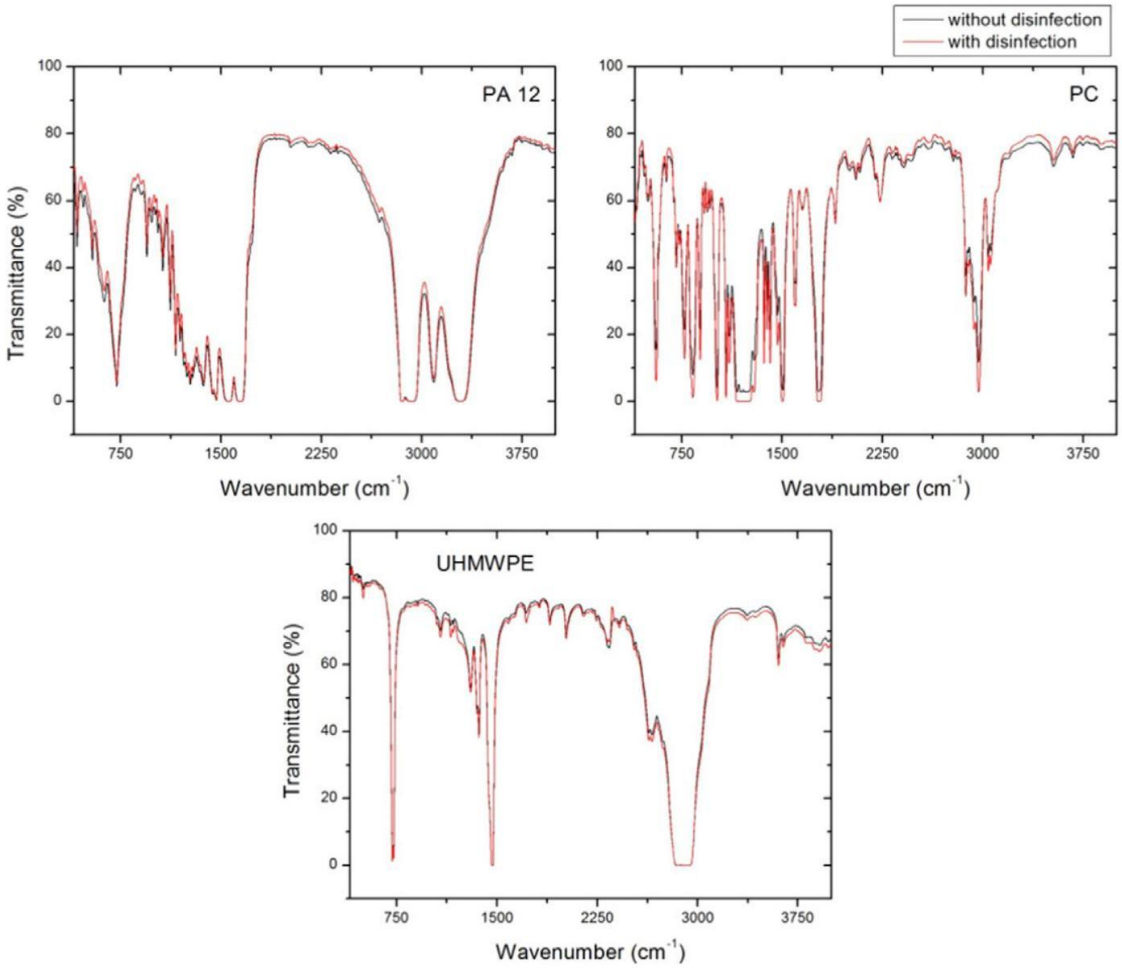

Fig. 3. FTIR spectra of PA 12, PC and UHMWPE: the FTIR spectra for each material without disinfection are shown in black and the FTIR spectra for films disinfected are shown in red.

by the processing pressure (62% reduction when pressure increases by a fourfold) and processing time (24% reduction) since a higher pressure/ cycle time translates into an increased particle compaction and coalescence, ultimately leading to a densification of the wick structure. Such densification should also lead to an improvement of the mechanical properties, as already concluded from Fig. 4. The processing temperature seems not to affect the porosity. Indeed, although higher temperatures lead to stronger structures (see Fig. 4), the effect seems not enough to promote a significant densification of the structure. On the other hand, no porosity differences are observed when different powder granulometries are used, except for the highest granulometry (G4), for which a reduction of about 20% is observed. In fact, it was observed that for the same mass of powder the volume occupied in the mould in the case of G4 was the smallest of all powders. Thus, the apparent density of G4 is the highest and hence the porosity should be the lowest, confirming the results. For the lower particle size powders the irregular shapes of the particles should facilitate their compaction, making the inter-particle space essentially independent of the particle size in the studied size range.

Table 2
Yield strength in compression and Young modulus of PC, UHMWPE and PA12 porous structures fabricated by sintering of compact wicks.

Polymer	PC	UHMWPE	PA12
Yield strength in compression (MPa)	2.7	0.6	0.9
Young modulus (MPa)	74.5	70.6	73.5

4.2.4. Permeability and mean pore radius

The permeability and mean pore radius of the PC structures were calculated by using the Darcy's law based model, Fig. 6. The mean pore radius is shown to decrease with the increase of cycle time (30%)

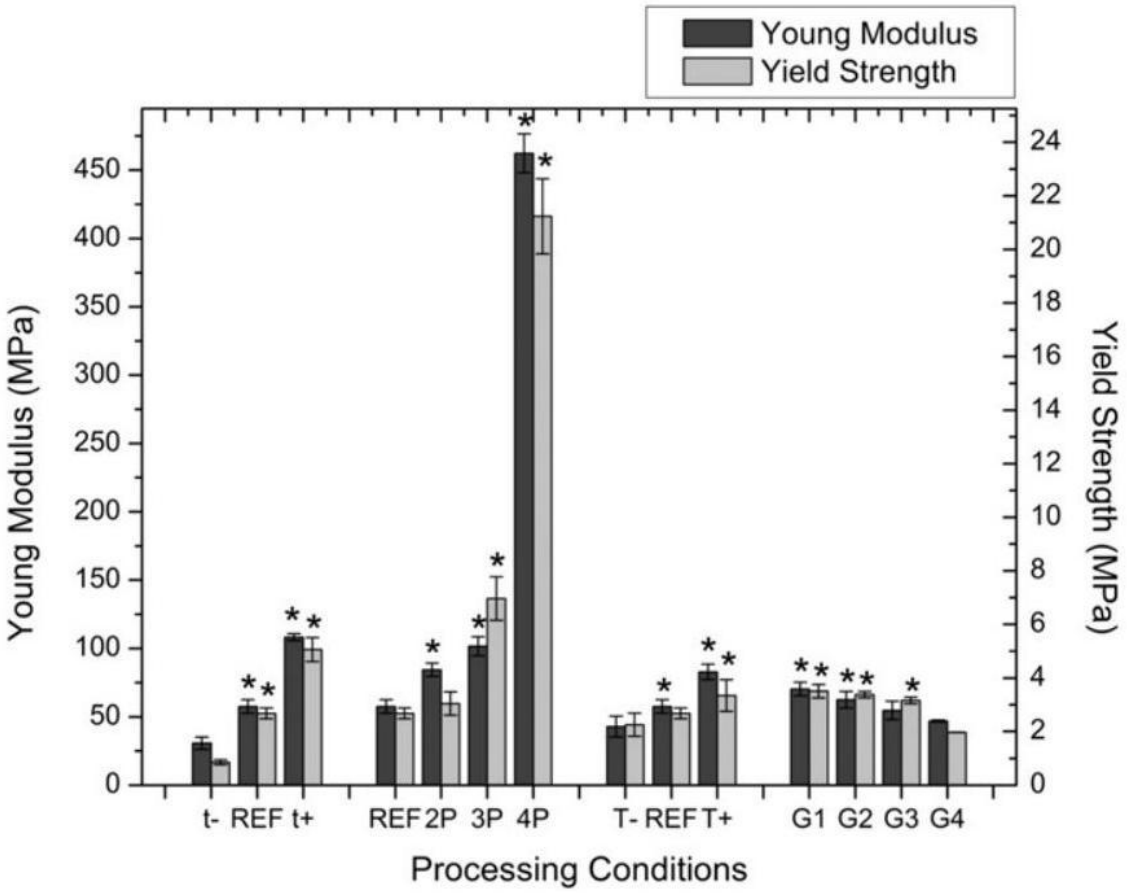

Fig. 4. Yield strength in compression and Young modulus of the wicks under uniaxial compression, as a function of the processing conditions. The assignment of a bar with "*" indicates that the difference between the Young modulus/yield strength value and the lowest value found on that group is statistically significant ($p < 0.05$).

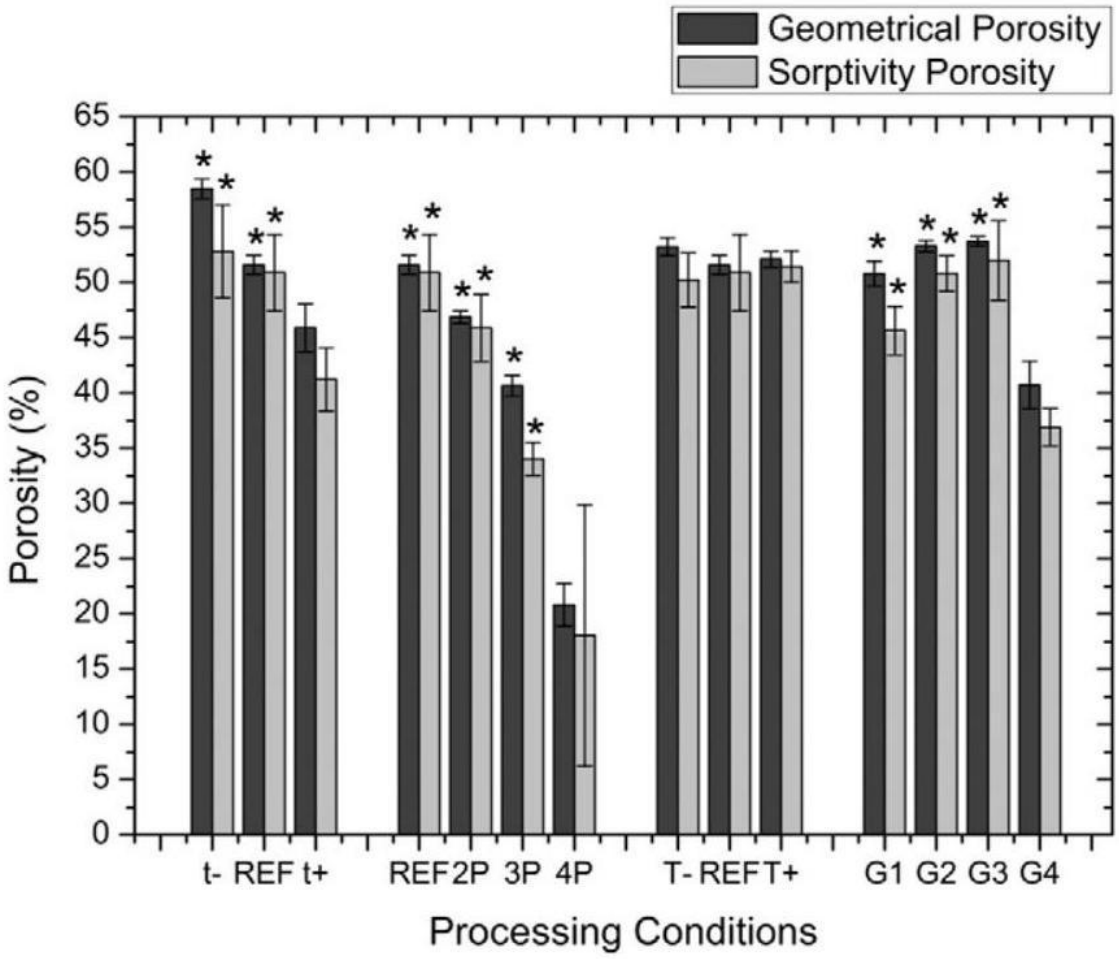

Fig. 5. Porosity obtained by the geometric and sorptivity methods. The assignment of a bar with "*" indicates that the difference between that porosity value and the lowest value found on that group is statistically significant ($p < 0.05$).
and processing pressure (55%), the same trend observed for porosity in Fig. 5. Furthermore, the mean pore radius slightly increases with the increase of the processing temperature (18%), even if porosity was shown to remain unaffected in these conditions (compare Figs. 5 and 6). An explanation could be that small pores collapse during the inter-particle bonding process for the highest temperatures leading to an increase of the mean pore radius, while not substantially affecting the total porosity. As for porosity, the increase of granulometry has a low impact on the mean pore radius, except for the highest granulometry (G4). Combining the results of Figs. 5 and 6 it can be concluded that the utilization of the G4 powder leads to a less porous structure but with a larger mean pore radius.

Permeability values are affected by larger errors, hence it was more difficult to obtain statistically significant differences with the processing conditions. However, permeability is shown to consistently decrease with the increase of the processing pressure (75%), in line with the

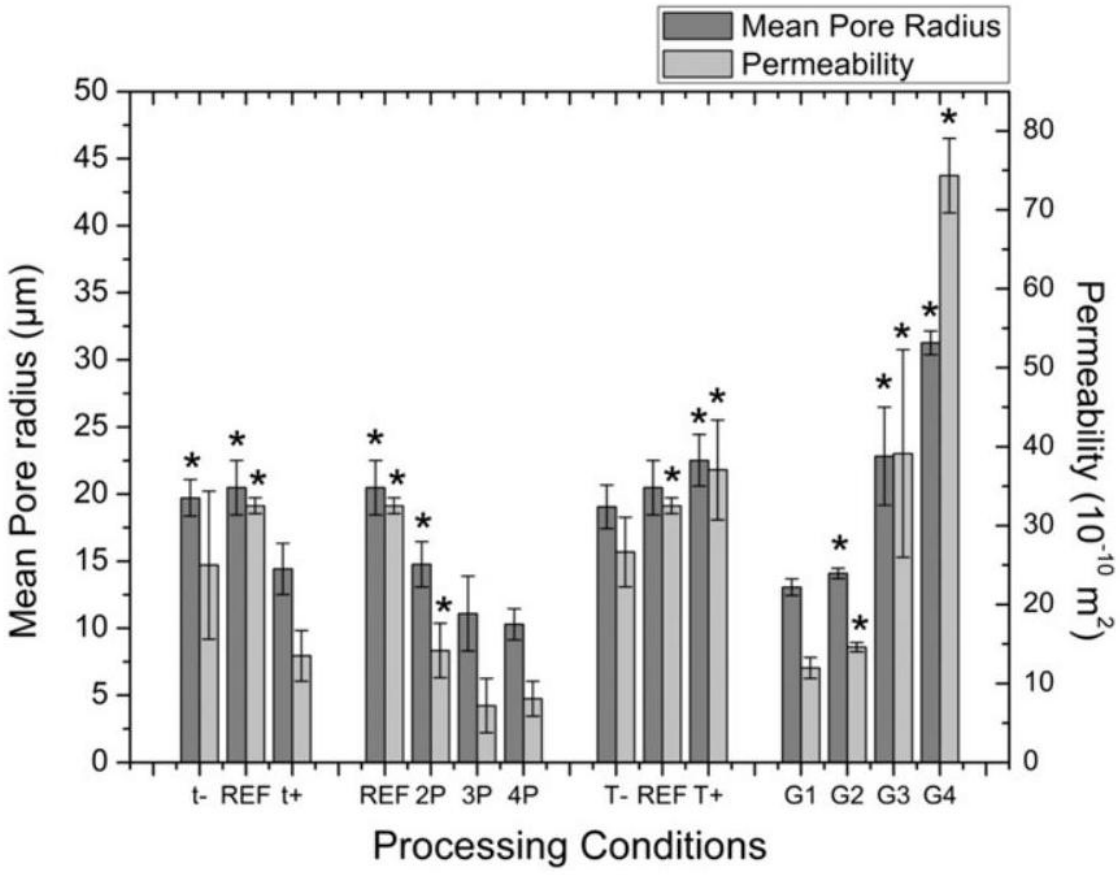

Fig. 6. Permeability (right) and mean pore radius (left) for PC wicks obtained using the model derived from the Darcy's law. The assignment of a bar with "*" indicates that the difference between that pore radius/permeability value and the lowest value found on that group is statistically significant ($p < 0.05$).
observed decrease of porosity and mean pore radius, as expected. Furthermore, the increase of PC granulometry has a strong effect on the permeability (fivefold increase), especially for the highest grain sizes, also in line with the increase of the mean pore radius and porosity. As for porosity and mean pore radius, the processing temperature seems to have only a minor effect on permeability. The average permeability values obtained for our wicks are of the order of those obtained by Masoodi [7] for PC, polyethylene and polypropylene wicks, even if higher average porosities (but lower pore radii) were obtained in the present work.

Mercury Intrusion Porosimetry (MIP)

Representative samples of the PC wicks were analysed by MIP, in order to assess the pore size distribution and also to validate the mean pore radii values obtained from the Darcy's law based model. Fig. 7 represents a typical MIP curve obtained for the PC wicking structures. A bimodal pore-size distribution is patent, characterized by the existence of a main pore distribution centered at $\sim 30\mu$ m and a residual percentage of pores with diameters ranging from 0.005 to 0.1μ m.

The porosity and average pore radii determined from MIP analysis are reported in Table 3, together with the same parameters determined from the Darcy's based model. The

excellent agreement among results obtained from both techniques validates the use of the model for these materials.

Scanning electron microscopy (SEM)

The SEM images obtained with the wicking materials show a wide pore radii distribution, corroborating the MIP results, Fig. 8a. Furthermore, besides the inter-particle pores, the wicks also present small pores within the own PC particles (Fig. 8b). It was confirmed that such pores were formed during the fragmentation process of the original PC pellets, carried out by milling in liquid nitrogen. These are blind pores, thus they are not accounted for by the Darcy model based procedure, although they are accounted by MIP, see the small pore distribution ($0.1 - 0.001\mu$ m) in Fig. 7. In Fig. 8b the necks formed among material particles and resulting from the sintering process are clearly visible.

Conclusions

The most influential processing parameter on the mechanical properties of the wicks is the processing pressure: an increase from 18.6 to 74.4 kPa leads to an eightfold increase of the yield strength, although

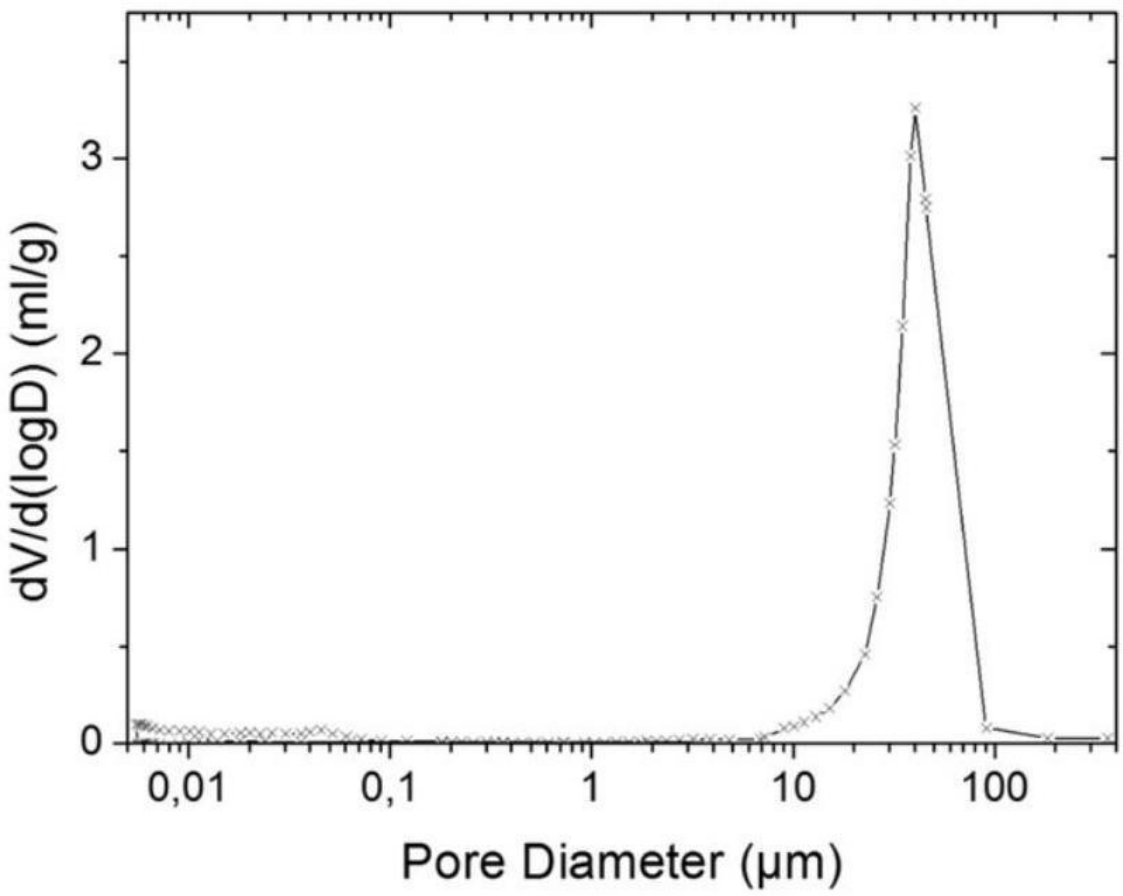

Fig. 7. Pore-size distribution determined by MIP for the REF condition, where a bi-modal distribution is identified.

Table 3
Representative porosities and mean pore radius obtained for PC wicks using Darcy's law and MIP results.

		Darcy's Law		MIP	
		Porosity (%)	Rw (μm)	Porosity (%)	Rw (μm)
Pressure (kPa)	REF	50	20	50	15
	4P	29	11	33	11
Temperature (°C)	T_-	50	19	48	17
	T_+	49	22	52	27
Cycle time (m)	REF	50	20	50	15
	t_+	40	14	44	13
Particle size (μm)	G1	50	23	49	17
	G4	48	33	31	36

at the expense of an unacceptable decrease of porosity (60%). However, the wicks produced with an intermediate pressure of 3 P (56 kPa) proved to display a good compromise between mechanical properties (yield strength increases by 150%) and porosity (porosity loss of 18%).

The processing time is also an important parameter, since an increase from 2.5 to 7.5 min led to a decrease of porosity and mean pore

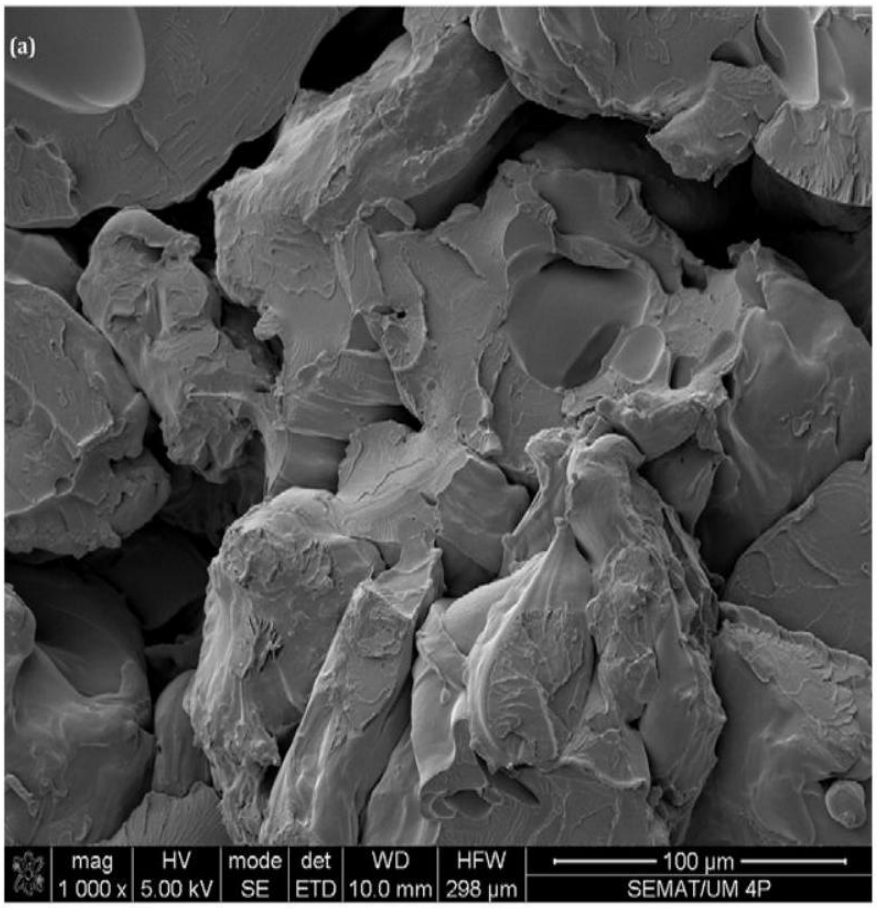
(a)
mag
1 000 x
HV
5.00 kV
mode
SE
det
ETD
WD
10.0 mm
HFW
298 µm
100 µm
SEMAT/UM 4P

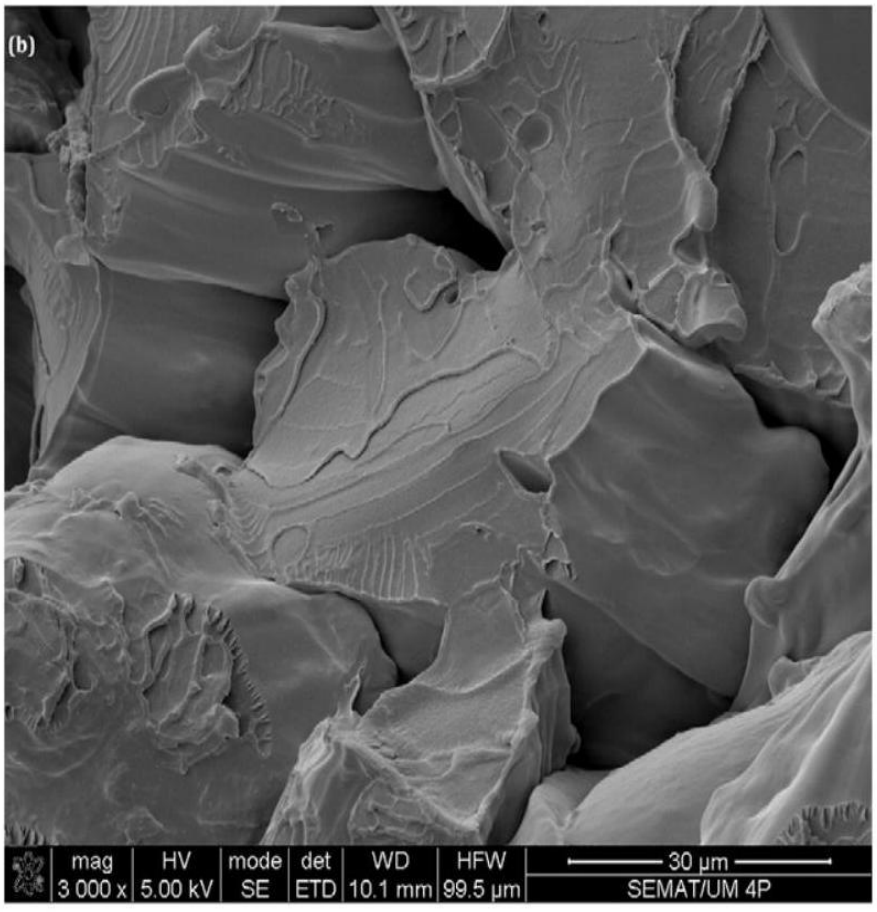
(b)
mag
3 000 x
HV
5.00 kV
mode
SE
det
ETD
WD
10.1 mm
HFW
99.5 µm
30 µm
SEMAT/UM 4P

Fig. 8. SEM images obtained with PC wicks: (a) different powder particles fused together, and (b) scan with a higher magnitude showing the micropores and necks. radius of about 25%, while temperature and powder grain size only have minor effects on the mechanical properties and porosity/mean pore radius (provided that powder grain size is controlled below 500μ m). The calculated permeability evolution correlates well with the porosity and mean pore radius evolution.

In conclusion, PC proved to be a suitable material for the fabrication of bio-electrode wicking structures. For that purpose, PC powders should be processed at 165 °C for 5 min , with an applied pressure of 3 P (56 KPa). Powder granulometry should be kept below 500μ m.

Acknowledgements

The authors gratefully acknowledge the Fundacão para a Ciência e Tecnologia, FCT (COMPETE Program) under the project FCOMP-010124 - FEDER-010190 (Ref. PTDC/SAU-ENB/116850/2010), FEDER, via FCT, under PEst-C/CTM/LA0025/2013 and PEst-C/EME/UI0285/2013 and MatePro Project, NORTE-07-0124-FEDER-000039, supported by the Programa Operacional Regional do Norte (ON.2). C.F. acknowledges discussions with M. Oliveira from Porto University, Portugal, and the revision of the document performed by P. Fiedler from the Technical University of Ilmenau, Germany.

References

[1] E. McAdams, Bioelectrodes, in: J.G. Webster (Ed.), Encyclopedia of Medical Devices and Instrumentation, Wiley, New York, 1988.
[2] C. Fonseca, J.P. Silva Cunha, R.E. Martins, V.M. Ferreira, J.P. Marques de Sá, M.A. Barbosa, A. Martins Silva, A novel dry active electrode for EEG recording, IEEE Trans. Biomed. Eng. 54 (2007) 162-165.
[3] A.R. Mota, L. Duarte, D. Rodrigues, A.C. Martins, A.V. Machado, F. Vaz, P. Fiedler, J. Haueisen, J.M. Nóbrega, C. Fonseca, Development of a quasi-dry electrode for EEG recording, Sensors Actuators A Phys. 199 (2013) 310-317.
[4] A. Searle, L. Kirkup, A direct comparison of wet, dry and insulating bioelectric recording electrodes, Physiol. Meas. 21 (2000) 271-283.
[5] D. Wu, F. Xu, B. Sun, R. Fu, H. He, K. Matyjaszewski, Design and preparation of porous polymers, Chem. Rev. 112 (2012) 3959-4015.
[6] V. Shkolnikov, D.G. Strickland, D.P. Fenning, J.G. Santiago, Design and fabrication of porous polymer wick structures, Sensors Actuators B Chem. 150 (2010) 556-563.
[7] R. Masoodi, K.M. Pillai, P.P. Varanasi, Darcy's law-based models for liquid absorption in polymer wicks, AIChE J. 53 (2007) 2769-2782.
[8] A. Siebold, M. Nardin, J. Schultz, A. Walliser, M. Oppliger, Effect of dynamic contact angle on capillary rise phenomena, Colloids Surf. A Physicochem. Eng. Asp. 161 (2000) 81-87.
[9] K. Leong, C. Cheah, C. Chua, Solid freeform fabrication of three-dimensional scaffolds for engineering replacement tissues and organs, Biomaterials 24 (2003) 2363-2378.
[10] D.W. Hutmacher, T. Schantz, K.W. Ng, S.H. Teoh, K.C. Tan, Mechanical properties and cell cultural response of polycaprolactone scaffolds designed and fabricated via fused deposition modeling, J. Biomed. Mater. Res. 55 (2001) 203-216.
[11] J.P. Kruth, G. Levy, R. Schindel, T. Craeghs, E. Yasa, Consolidation of polymer

powders by selective laser sintering, Proceedings of the 3rd International Conference on Polymers and Moulds Innovations, 2008, pp. 15-30.
[12] H. Seitz, W. Rieder, S. Irsen, B. Leukers, C. Tille, Three-dimensional printing of porous ceramic scaffolds for bone tissue engineering, J. Biomed. Mater. Res. B Appl. Biomater. 74 (2005) 782-788.
[13] R.K. Chu, H.E. Naguib, N. Atalla, Synthesis and characterization of open-cell foams for sound absorption with rotational molding method, Polym. Eng. Sci. 49 (2009) 1744-1754.
[14] R.C. Thomson, A.K. Shung, M.J. Yaszemski, A.G. Mikos, Polymer scaffold processing, in: R. Lanza, R. Langer, J. Vacanti (Eds.), Principles of Tissue Engineering, second ed.Academic Press, 2000, pp. 251-262.
[15] J.H. de Groot, R. deVrjer, A.J. Pennings, J. Klompmaker, R.P.H. Veth, H.W.B. Jansen, Use of porous polyurethanes for meniscal reconstruction and meniscal prostheses, Biomaterials 17 (1996) 163-173.
[16] A.S. Patil, Antimicrobial sintered porous plastic filter, U.S. Patent 6,540,916 (2003).
[17] M.W. Smith, D. Fullerton, Sintered porous plastic material, US Patent 6,399,188 (2002).
[18] J.P. Wingo, M.E. Witover, M. Guoqiang, A. Maertens, G. Fullerton, Haldopoulos II Tan TH, Reed DB, Sintered polymeric materials and applications thereof. U.S. Patent 8,141,717 (2012).
[19] S. Hanbir, J.P. Jog, Sintering of ultra high molecular weight polyethylene, Bull. Mater. Sci. 23 (2000) 221-226.
[20] P. Fiedler, S. Biller, C. Fonseca, F. Vaz, S. Griebel, F. Zanow, J. Haueisen, Signal quality of titanium and titanium nitride coated dry polymer electrodes, Biomed. Eng./ Biomed. Tech. 57 (Suppl. 1) (2012) 1083.
[21] J. Richardson, IR Spectroscopy Tutorial, 2011. (accessed 31 Out 2013).
[22] X. Wu, C. Wu, G. Wang, P. Jiang, Z. Jianqiang, A crosslinking method of UHMWPE irradiated by electron beam using TMPTMA as radiosensitizer, J. Appl. Polym. Sci. 127 (2012) 111-119.